Supporting Information

Interactions of 1-hydroxypyrene with bovine serum albumin: Insights from multi-spectroscopy, docking and molecular dynamics simulation methods

Jing Zhang[a], Weixiao Chen[a,b], Bowen Tang[c], Wei Zhang[a], Linfeng Chen[a], Ying Duan[a],

Yuxiu Zhu[a], Yaxian Zhu[d], Yong Zhang[a,e*]

[a]State Key Laboratory of Marine Environmental Sciences of China (Xiamen University), College of Environment and Ecology, Xiamen University, Xiamen 361102, China

[b] College of Urban and Environmental Sciences, Peking University, Beijing 100871, China

[c] College of Pharmaceutical Sciences, Xiamen University, Xiamen 361102, China

[d] Department of Chemistry, College of Chemistry and Chemical Engineering, Xiamen University, Xiamen 361005, China

[e] Zhangzhou Institute of Technology, Zhangzhou 363000, China

*E-mail address: yzhang:xmu.edu.cn

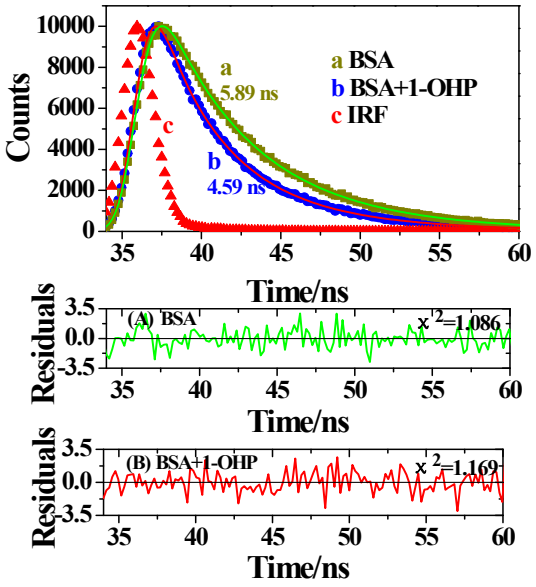

Fig. S1. Fluorescence decay curves of BSA in the absence (a) and presence of 1-OHP (b) and the obtained instrumental response function (IRF) (c). Insets (A) and (B) show a random distribution of the weighted residuals around zero of the two systems. $C_{1\text{-}OHP} = C_{BSA} = 5.0\times10^{-6}$ mol L^{-1}

Calculation of the dynamic and static quenching constant of 1-OHP and BSA

To extract a more quantitative view of the mixed quenching mechanism, the data was analyzed using the Eq. (S1) [1]:

$$F_0 / F = (1 + K_D[Q])(1 + K_S[Q]) = K_D K_S [Q]^2 + (K_D + K_S)[Q] + 1 \quad \text{(S1)}$$

F_0 and F represent the fluorescence intensity in the absence and presence of the quencher (1-OHP in this case), respectively; K_S, K_D are the static and dynamic quenching constants, respectively; Q is the concentration of the quencher. It's calculated that $K_D \cdot K_S$ equals 3.12×10^9 and $(K_D + K_S)$ equals 1.16×10^5. Therefore, the

possible solutions, 7.48×10^4 and 4.14×10^4, are the values of K_D and K_S. Additional analysis is followed to resolve the definitive value of each. Different from the static quenching, where $\tau_0 / \tau = 1$. The fluorescence intensity (F) and lifetime (τ) in dynamic quenching of the protein is described by Eq. (S2) [1,2]:

$$F_0 / F = \tau_0 / \tau = 1 + K_q \tau_0 [Q] = 1 + K_D [Q] \quad \text{(S2)}$$

In Eq (S2), τ_0 is the average lifetime of BSA in the absence of 1-OHP. Quenching data of BSA has been fit to the Stern–Volmer plot, (τ_0 / τ) vs. $C_{1\text{-}OHP}$ (see Fig. S2). From the slope of the linear function, namely the dynamic quenching constant, K_D, is calculated to be 4.35×10^4 L mol^{-1}. 4.14×10^4 and 4.35×10^4 L mol^{-1}are on the same order of magnitude and strikingly similar and as a result, K_D is determined to be 4.14×10^4 L mol^{-1}, giving K_S a value of 7.48×10^4 L mol^{-1}.

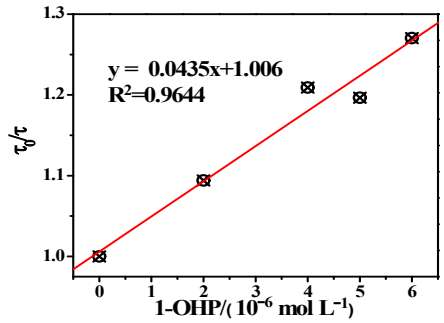

Fig. S2. Stern–Volmer plot of (τ_0/τ) vs. $C_{1\text{-}OHP}$ in Tris-HCl buffer (pH 7.40). τ_0 is the lifetime of BSA without 1-OHP, and τ is the lifetime in the presence of 0, 0.2, 0.4 , 0.5, 0.6×10^{-5} mol L^{-1} 1-OHP, $C_{BSA} = 5.0\times10^{-6}$ mol L^{-1}.

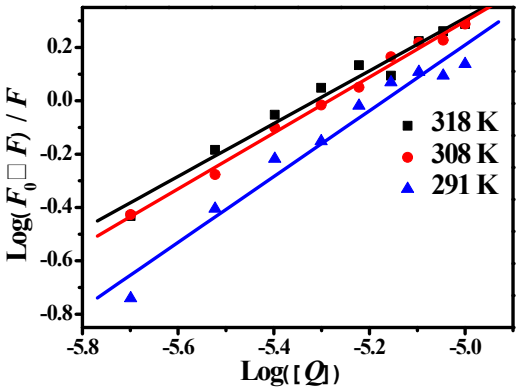

Fig. S3. The relationship between log $(F_0 - F)$ /F and log [Q] for BSA-1-OHP systems at 291, 308 and 318 K: C_{BSA} = 5.0×10^{-6} mol L^{-1}, $C_{1\text{-OHP}}$ = (0, 0. 3, 0.4, 0.5, 0.6, 0.7, 0.8, 0.9, 1.0) ×10^{-5} mol L^{-1}, λ_{em} = 341 nm

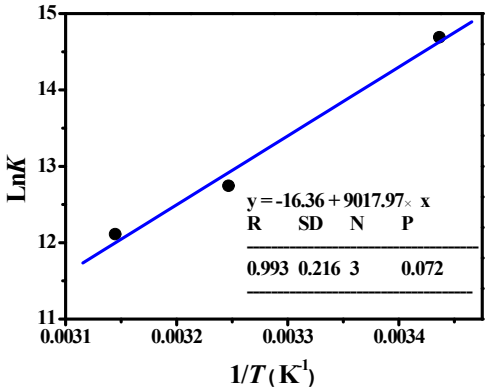

Fig. S4. Van't Hof plot for the BSA-1-OHP system

Calculation of the Binding distance from BSA to 1-OHP using FERT The efficiency of energy transfer (E) between the donor, Trp residues of BSA and acceptor, 1-OHP can be calculated by applying equation (S3) [3]:

$$E = 1 - \frac{F}{F_0} = \frac{R_0^6}{R_0^6 + r^6} \quad \text{(S3)}$$

In the equation (S3), F and F_0 are the fluorescence intensity of BSA in the presence and absence of 1-OHP. r is the distance between the donor and acceptor. R_0 is the Förster radius (measured in Å), the critical distance at which the transfer efficiency equals 50%, is given by the following equation:

$$R_0^6 = 8.79 \times 10^{-25} K^2 n^{-4} \phi J \quad \text{(S4)}$$

Where K is the orientation factor related to the geometry of the donor-acceptor dipole, n is the refractive index of medium, φ is the fluorescence quantum yield of the donor, and J expresses the degree of spectral overlap between the donor emission and the acceptor absorption, in unit of L mol^{-1} cm^3, which is calculated by the following equation：

$$J = \frac{\int_0^\infty F(\lambda)\varepsilon(\lambda)\lambda^4 d\lambda}{\int_0^\infty F(\lambda) d\lambda} \quad \text{(S5)}$$

$F(\lambda)$ is the corrected fluorescence intensity of the donor in the wavelength range from λ to $\lambda + \Delta\lambda$ *and* $\varepsilon(\lambda)$ is the molar absorption coefficient of the acceptor at wavelength λ, in unit of L mol^{-1} cm^{-1}.

In our case, k^2 = 2/3, ϕ (BSA) = 0.15, and N = 1.336 [4]. At the same concentration of BSA and 1-OHP of 5×10^{-6} mol L^{-1}, E was determined to be 0.40.

The overlap integral, J, can be evaluated by integrating the spectra in Fig. 6 according to Eq. (S5), and was calculated to be 1.37×10^{-14} cm^3 L mol^{-1}. Fitting the J and E values to Eq. (S3)—(S4), the values of the parameters were listed in Table S1.

Table S1 The calculated parameters of FRET between 1-OHP and BSA;

$C_{BSA} = C_{1\text{-}OHP} = 5.0\times10^{-6}$ mol L^{-1}

	J (cm^3 L mol^{-1})	E (%)	R_0 (nm)	r (nm)
1-OHP-BSA	1.37×10^{-14}	40.0	2.69	2.88

Interpretations for the colors in the molecular docking results shown in Fig.7 and Fig. 9 For the molecular docking results shown in Fig. 7: (A). TRP 134 and TRP 213 residues are shown as yellow surface; 1-OHP is showed as magenta; BSA is shown as cyan; (B). the C atoms, H atom and O atom of 1-OHP are shown as green, red and gray, respectively; BSA is shown as chainbows; (C). for amino acid residues, the C atoms, H atoms, O atoms, and S atoms are shown as magenta, gray, blue, red and orange, respectively; and the C atoms, H atom and O atom of 1-OHP are shown as green, red and gray, respectively; BSA is shown as cyan.

For the molecular dynamic results shown in Fig. 9: for the amino acid residues within a distance of 5 Å approximately 1-OHP, the C atoms, H atoms, O atoms, and S atoms are shown as magenta, gray, blue, red and orange, respectively; and the C atoms, H atom and O atom of 1-OHP are shown as green, red and gray, respectively.

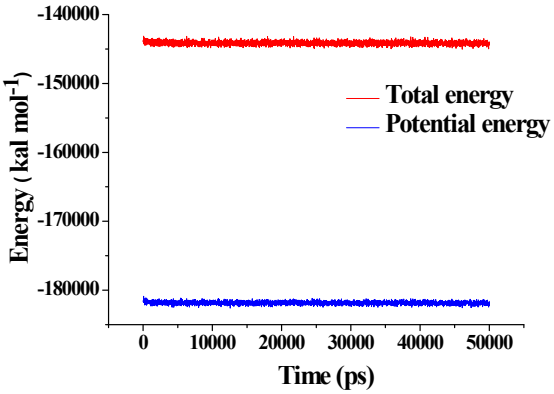

Fig. S5. The potential energy (blue line) and total energy (red line) of the 1-OHP-BSA complex.

(A)

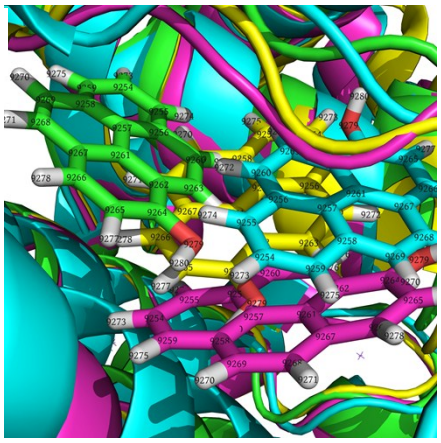

(B)

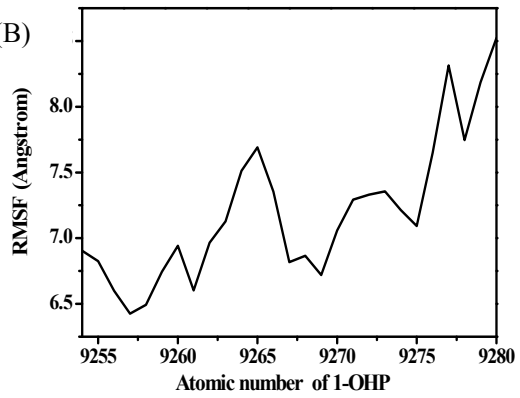

Fig. S6. (a) The overlapping graph of the four snapshots of 1-OHP-BSA complex at 15 ns, 25 ns, 30 ns and 40 ns. (b) The average root mean square fluctuation (RMSF) of each atom of 1-OHP during the 2000 flames simulations.

a: For the snapshot at 15 ns, 20 ns, 30 ns and 40 ns, BSA is shown as green, cyan, magenta and yellow, and the C atoms of 1-OHP are also shown as green, cyan, magenta and yellow, respectively; and the O atom and H atom of 1-OHP are all shown as red and gray, respectively. For the four snapshots, the atoms of 1-OHP are all labeled as 9294~9280. b: the RMSF values represent the position shifts of each atoms of 1-OHP during the 2000 flame simulations, and the 2000 flames are the sum of every 500 frames before 15 ns, 20 ns, 30 ns and 40 ns.

Table S2 Conformational changes of 1-OHP at four snapshots as calculated using AmberTools 15

Time (ns)[a]	RMSD of 1-OHP[a,b] (Å)	Angle of –OH group of 1-OHP[a] (°)	Dihedral angle between the –OH group and the four-fused ring group of 1-OHP[a] (°)
15	10.32	102.12	-170.77
20	13.14	104.74	102.19
30	0	110.02	165.69
40	7.45	104.66	178.55

a The obtained values are the average values of every 500 frames before 15 ns, 20 ns, 30 ns and 40 ns, respectively.

b The RSMD represents the relative position shifts of 1-OHP at different time, setting the position of 1-OHP at 30 ns as a reference. Notably, the RMSD here is calculated as the no-fit RMSD, which considers the translations and rotations of 1-OHP.

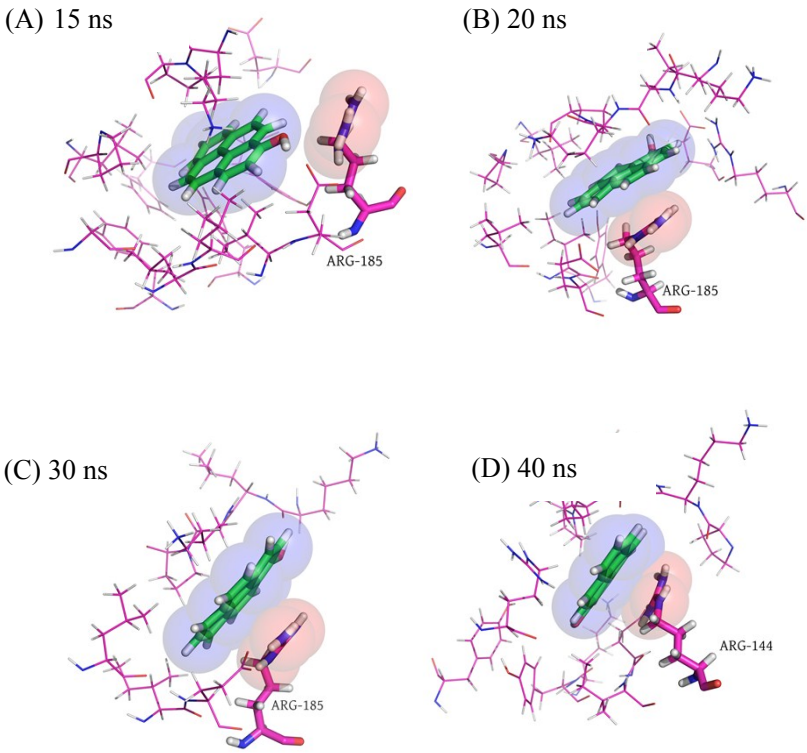

Fig. S7. Binding modes of 1-OHP with BSA at 15 ns (A), 20 ns (B), 30 ns (C), and 40 ns (D) in the MD simulation

The cation-π interactions formed between the positively charged nitrogens from the side chain of ARG185 (B,C) or ARG144 (D) and the large π-system from 1-OHP at 20 ns, 30 ns and 40 ns; the electron cloud of 1-OHP and the side chain of ARG185 (A, B, C) or ARG144 (D) are shown as blue sphere and orange sphere, respectively; the amino acid residues within a distance of 5 Å approximately 1-OHP are shown as lines, except for ARG185 (A, B, C) or ARG144 (D) shown as sticks; the color of 1-OHP and the amino acid residues are shown in the same way as Fig. 9

Table S3 The geometry of hydrogen bonds formed between 1-OHP and BSA during the simulation process [a]

Acceptor [b]	Donor H [b]	Donor [b]	Occupancy [c] (%)	Averaged Distance (Å)	Averaged Angle (°)
GLU 182:OE1	1-OHP:H10	1-OHP:O1	34.42	2.63	165.42
GLU 182:OE2	1-OHP:H10	1-OHP:O1	17.24	2.63	165.42
1-OHP:O1	TYR 160:HH	TYR 160:OH	2.65	2.81	157.87
GLU 140:OE2	1-OHP:H10	1-OHP:O1	2.49	2.66	163.94
LYS 114:O	1-OHP:H10	1-OHP:O1	1.57	2.73	158.51
LEU 115:O	1-OHP:H10	1-OHP:O1	0.82	2.73	159.18
TYR 160:OH	1-OHP:H10	1-OHP:O1	0.46	2.85	161.84
PRO 117:O	1-OHP:H10	1-OHP:O1	0.31	2.77	157.21
LIG 584:O1	LYS 116:HZ3	LYS 116:NZ	0.20	2.92	145.78
LIG 584:O1	LYS 116:HZ1	LYS 116:NZ	0.18	2.91	151.25
LIG 584:O1	LYS 116:HZ2	LYS 116:NZ	0.15	2.89	155.85
LIG 584:O1	ARG 185:HH11	ARG 185:NH1	0.13	2.93	161.57
PRO 113:O	1-OHP:H10	1-OHP:O1	0.11	2.76	162.98

[a] For the hydrogen bonds, the distance between the acceptor and donor heavy atoms is less than 3.5 Å. The angles of acceptor and donor diatomic groups are no less than 120°.

[b] The first one character of the atom name consists of the chemical symbol for the atom type. All the atom names beginning with ‘‘H’’ are hydrogen atoms; ‘‘N’’ indicates a nitrogen and ‘‘O’’ indicates oxygen. The next character is the remoteness indicator code, which is transliterated according to: “E” stands for (~) “ε”; “Z”~“ζ”; “H”~“η”.

[c] The hydrogen bond occupancy is calculated as the ratio of conformations with hydrogen bonds to

the total 5000 conformations.

Table S4 Secondary structural alterations of BSA at four snapshots as calculated by AmberTools15 using DSSP method

Time[a] (ns)	Parallel Beta-sheet[b] (%)	Anti-parallel Beta-sheet[b] (%)	3-10 helix[b] (%)	Alpha helix[b] (%)	Pi(3-14) helix[b] (%)	Turn[b] (%)	Bend [b] (%)
15	0	0	2.43	68.69	0.06	10.25	5.88
20	0	0	2.31	68.74	0.09	10.33	5.91
30	0	0	2.15	68.73	0.12	10.48	5.99
40	0	0	2.16	68.58	0.12	10.60	5.98

a The obtained values are the average values of every 500 frames before 15 ns, 20 ns, 30 ns and 40 ns, respectively.

b There could be many possible reasons for the slight difference in the secondary structural data calculated here from that derived from CD experiment: 1) The CD data corresponds to solution state, whereas the calculated data using X-ray structure corresponds to crystal state, it might possible that the conformation adopted by our system in solution state is different from the crystal state; 2) Affects of the CD operating conditions (during the spectral measurements and during deconvolution); 3) Affects of the computing methods employed in the theoretical calculation part, etc.

Table S5 Binding free energies (kcal mol^{-1}) obtained by the MM-PBAS method in every 5 ns MD simulation

Time/ ns	ΔE_{vdw}[a]	ΔE_{ele}[b]	ΔE_{polar}[c]	$\Delta E_{nonpolar}$[d]	$\Sigma E_{nonpolar}$[e]	ΣE_{polar}[f]	ΔE_{bind}[g]
1~5	-24.52	-13.53	21.16	-2.95	-27.47	7.63	-15.49
5~10	-26.05	-3.21	14.09	-2.92	-28.97	10.88	-13.51
10~15	-21.20	-20.34	26.11	-2.83	-24.03	5.77	-16.90
15~20	-22.60	-11.04	18.51	-2.80	-25.40	7.47	-15.70
20~25	-23.64	-9.35	17.29	-2.76	-26.40	7.94	-16.40
25~30	-22.62	-18.67	24.78	-2.60	-25.21	6.11	-18.15
30~35	-23.72	-18.83	24.32	-2.69	-26.40	5.48	-19.71
35~40	-25.59	-13.53	21.16	-2.75	-28.34	7.63	-14.12
40~45	-22.83	-21.15	25.54	-2.56	-25.40	4.38	-21.11
45~50	-22.10	-18.02	24.45	-2.73	-24.82	6.43	-16.21
Average[h]	-23.98±2.46	-18.28±10.00	27.66±5.95	-2.72±0.17	-	-	-17.32±4.23

[a] Van der Waals energy, calculated using the MM force field;

[b] Electrostatic energy, calculated using the MM force field;

[c] Polar solvation free energy, calculated using the PB equation;

[d] Nonpolar solvation free energy, calculated using an empirical model;

[e] $\Sigma E_{nonpolar}=\Delta E_{vdw}+\Delta E_{nonpolar}$;

[f] $\Sigma E_{polar}=\Delta E_{ele}+\Delta E_{polar}$;

[g] $\Delta E_{bind}=\Delta E_{gas}+\Delta E_{sol}=(\Delta E_{vdw}+\Delta E_{ele})+(\Delta E_{polar}+\Delta E_{nonpolar})$;

[h]The average values of the decomposition of binding free energies during the 50 ns simulations, calculated using the MM force field.

Table S6 The average values of the decomposition of binding free energies (kcal mol^{-1}) of key residues

Residues	ΔE_{vdw}[a]	ΔE_{ele}[b]	ΔE_{polar}[c]	$\Delta E_{nonpolar}$[d]	ΔE_{bind}[e]
PRO 113	-0.25	-0.02	0.10	0.00	-0.17
LYS 114	-0.46	0.04	0.73	0.00	0.31
LEU 115	-0.76	-0.13	0.92	0.00	0.04
LYS 116	-2.01	-1.48	2.98	0.00	-0.50
PRO 117	-1.60	0.05	0.46	0.00	-1.09
PRO 119	-0.18	0.00	0.10	0.00	-0.08
LEU 122	-0.34	-0.04	0.14	0.00	-0.25
TYR 137	-0.27	-0.03	0.28	0.00	-0.01
GLU 140	-0.54	-0.59	0.79	0.00	-0.34
ILE 141	-0.27	0.01	-0.03	0.00	-0.29
ARG 144	-0.86	-0.38	1.99	0.00	0.75
TYR 160	-0.26	-0.11	0.54	0.00	0.17
LEU 178	-0.36	-0.07	0.14	0.00	-0.28
ILE 181	-0.63	0.12	0.01	0.00	-0.49
GLU 182	-0.14	-4.12	4.60	0.00	0.34
ARG 185	-1.91	-0.73	2.22	0.00	-0.42

[a-e] calculated in the same way as illustrated in Table S3

References:

1. J. R. Lakowicz, *Principles of fluorescence spectroscopy*, Springer Science & Business Media, 2013.
2. B. P. Pahari, S. Chaudhuri, S. Chakraborty and P. K. Sengupta, *J. Phys. Chem. B*, 2014, **119**, 2533-2545.
3. T. Förster, *Delocalized excitation and excitation transfer*, Florida State University, 1965.
4. H. Xu, Q. Liu and Y. Wen, *Spectrochim. Acta A.*, 2008, **71**, 984-988.